Since January 2020 Elsevier has created a COVID-19 resource centre with free information in English and Mandarin on the novel coronavirus COVID-19. The COVID-19 resource centre is hosted on Elsevier Connect, the company's public news and information website.

International Journal of Pharmaceutics 608 (2021) 121122

Contents lists available at ScienceDirect

International Journal of Pharmaceutics

journal homepage: www.elsevier.com/locate/ijpharm

Inhaled Edoxaban dry powder inhaler formulations: Development, characterization and their effects on the coagulopathy associated with COVID-19 infection

Md Abdur Rashid [a], Saiqa Muneer [b], Jayanti Mendhi [c], Mohammad Zaidur Rahman Sabuj [d], Yahya Alhamhoom [a], Yin Xiao [c,e], Tony Wang [f], Emad L. Izake [b], Nazrul Islam [d,g,*]

[a] Department of Pharmaceutics, College of Pharmacy, King Khalid University, Abha, Aseer 62529, Saudi Arabia
[b] School of Chemistry and Physics, Faculty of Science, Queensland University of Technology, Brisbane, Queensland, Australia
[c] Queensland University of Technology, Centre for Biomedical Technology, Brisbane, Queensland, Australia
[d] Pharmacy Discipline, School of Clinical Sciences, Faculty of Health, Queensland University of Technology, Brisbane, Queensland, Australia
[e] Australia-China Centre for Tissue Engineering and Regenerative Medicine, Queensland University of Technology, Brisbane, Queensland, Australia
[f] Central Analytical Research Facility, Institution for Future Environment, Queensland University of Technology, Brisbane, Queensland, Australia
[g] Centre for Immunology and Infection Control (CIIC), Queensland University of Technology (QUT), Brisbane, Queensland, Australia

ARTICLE INFO

Keywords:
Edoxaban
Dry powder inhaler formulation
Pulmonary drug delivery venous thromboembolism
FPF
COVID-19
Coagulation

ABSTRACT

Herein, we demonstrated the development and characterization of a dry powder inhaler (DPI) formulation of edoxaban (EDX); and investigated the in-vitro anticoagulation effect for the management of pulmonary or cerebral coagulopathy associated with COVID-19 infection. The formulations were prepared by mixing the inhalable micronized drug with a large carrier lactose and dispersibility enhancers, leucine, and magnesium stearate. The drug-excipient interaction was studied using X-Ray diffraction (XRD), Fourier transform infrared spectroscopy (FTIR), differential scanning calorimetry (DSC) and thermogravimetric analysis (TGA) methods. The drug and excipients showed no physical inter particulate interaction. The in-vitro drug aerosolization from the developed formulation was determined by a Twin Stage Impinger (TSI) at a flow rate of 60 ± 5 L /min. The amount of drug deposition was quantified by an established HPLC-UV method. The fine particle fraction (FPF) of EDX API from drug alone formulation was 7%, whereas the formulations with excipients increased dramatically to almost 7-folds up to 47%. The developed DPI formulation of EDX showed a promising in-vitro anticoagulation effect at a very low concentration. This novel DPI formulation of EDX could be a potential and effective inhalation therapy for managing pulmonary venous thromboembolism (VTE) associated with COVID-19 infection. Further studies are warranted to investigate the toxicity and clinical application of the inhaled EDX DPI formulation.

1. Introduction

Edoxaban is a non-vitamin K antagonist, direct oral anti-coagulant (DOACs) and anti-thrombin drug (Matsushima et al., 2013). Edoxaban (EDX) was developed as a selective factor Xa-inhibitor which is used as an alternative to vitamin K antagonists such as warfarin to surmount the adverse effects during the prevention and treatment of venous thromboembolism (VTE) in patients with atrial fibrillation (AF) (Kearon et al., 2012). It overcomes undesirable pharmacokinetics and pharmacodynamic properties associated with orally administered warfarin such as the delayed onset of action, narrow therapeutic window, variable pharmacological response, and various drug-drug and drug-food interactions (Wells et al., 1994). A single dose of EDX reaches the peak plasma concentration after 1–2 hr of administration, followed by biphasic decline in healthy individuals. In addition, its elimination half-life is 10–14 hr with an oral bioavailability of 62% (Parasrampuria and Truitt, 2016). Relative to warfarin, EDX needs less monitoring and dietary conditions, a wide therapeutic window and reduced overall medication associated costs (Ferreira and Mirco, 2015). Recently, edoxaban's clinical application has been extended to manage pulmonary

* Corresponding author at: Pharmacy Discipline, School of Clinical Sciences, Faculty of Health, Queensland University of Technology, Brisbane, Queensland, Australia.
E-mail address: nazrul.islam@qut.edu.au (N. Islam).

https://doi.org/10.1016/j.ijpharm.2021.121122
Received 8 July 2021; Received in revised form 17 September 2021; Accepted 20 September 2021
Available online 21 September 2021

coagulopathy in some patients infected with COVID-19 coronavirus.

COVID-19 pandemic has led to a severe health catastrophe as the mortality rate reaches millions of people due to lung infection and thromboembolism and caused an unbearable economic burden globally. It has been observed that pulmonary coagulopathy is common in patients with deteriorated lung function due to the deadly infection caused by coronavirus (Costanzo et al., 2020; Flam et al., 2021). Since no clear mechanism explains the development of pulmonary coagulopathy due to COVID 19 infection, the application of anticoagulant is a must during COVID-19 treatment. Recently, Rentsch et al. (2021) demonstrated that the initial launch of prophylactic anticoagulant therapy compared with no anticoagulation treatment amongst patients with COVID-19 was linked with a reduced risk of mortality and no increased risk of serious bleeding events. This finding provides a real-world proof of concept for the use of anticoagulants as an initial treatment along with other medications for treating COVID-19 patients (Fogarty et al., 2020). The promising clinical evidence suggests that heparin-like molecules may be a potential drug to treat COVID-19 infection-related pulmonary coagulopathy (Hippensteel Joseph et al., 2020; Tang et al., 2020) and administration of anticoagulants could be a reliable and effective treatment option for COVID-19 patients suffering from VTE (Kartsios et al., 2021). It has been reported that the patients suffering from COVID-19 infections developed cerebral venous thrombosis along with pulmonary thromboembolism, and oral administration of EDX (60 mg/day) reduced thrombosis (Sugiyama et al., 2020). Switching of warfarin patients to EDX was found safe for COVID-19 related pulmonary thromboembolism (Patel et al., 2021). Flam et al. demonstrated that oral delivery of DOACs is not helpful as a potential therapy against coagulopathy associated with severe COVID-19 (Flam et al., 2021). Therefore, alternative delivery of anticoagulants is paramount to combat the pulmonary coagulopathy associated with the infection caused by COVID-19. Very recently, Islam and Rahman (Islam and Rahman, 2021) suggested that the lung delivery of drugs would be beneficial for the management of various complications associated with COVID-19 infection.

Pulmonary route of anticoagulant delivery would provide a promising strategy to overcome challenges associated with oral administration of anticoagulant. Pulmonary administration provides direct access of drug to the target site and has a rapid onset of action that reduces the total administered dose substantially as compared to the oral route of administration. In addition, it overcomes poor solubility, lower bioavailability, and serious dose-related gastrointestinal bleeding. Inhaled delivery of drugs from DPI, metered-dose inhaler (MDI) and nebulizers are well established for various disorders, especially lung diseases. This study is focused on the development of EDX DPI formulation, which consists of drug alone or mixed with large carrier particles (lactose) (Prime et al., 1997), which helps improve the powder flow properties (Chan et al., 1997), as the inhalable micronized drug particles (<5μm) are highly cohesive. Upon inhalation, the drug particles detach from the surface of large carrier particles and get into the lung along with the inhaled air, whereas the carrier particles deposit in the mouth or upper respiratory tract.

The present study aims at the development of EDX DPI formulation suitable for delivery via lungs for the management of pulmonary or cerebral thromboembolism associated with COVID 19 infection. We first time demonstrated the DPI formulation of EDX intended to direct delivery into deep lungs. The main objective of this study is to achieve the maximum therapeutic effect by administering a low dose of EDX from the inhaled formulation and to reduce the dose-related complications. We developed a DPI formulation of EDX by using inert excipients, characterized the formulations for in-vitro aerosolization and reported the in-vitro anticoagulation effect.

2. Materials and methods

2.1. Materials

Edoxaban tosylate monohydrate (Fig. 1) was obtained from Merck (United States) (Cas Number: 1229194-11-9, molecular weight of 738.29. α-Lactose monohydrate (Inhalation grade; Inhalac 120) was gifted by Meggle GmbH (Wasserburg, Germany). L-leucine, magnesium stearate (Mg-St), hard gelatin capsules (size 3), DMSO, phosphate buffered saline (PBS), and $CaCl_2$ were purchased from Sigma-Aldrich (Germany).

2.2. Micronization of EDX particles and size measurement

Utilizing a mortar and pestle, API of EDX was crushed to produce inhalable size particles (<5 μm) (Islam et al., 2004a). The size of the micronized particles was evaluated using the laser diffraction technique by Malvern Master sizer. Small amount of EDX powder was suspended in 10 mL of water and sonicated for 5 min. The concentrated suspension was added into the dispersion unit stirring at 2200 rpm until the obscuration reaches the required level. The refractive index used was 1.63 and absorption index was 1.2. The mean volume diameter (D [4,3]) were used as the major particle sizing parameters using the laser diffraction particle sizing technique and characterize the particle size distributions. The measurement was taken in triplicate.

2.3. Formulation blends and homogeneity test

The DPI formulations of EDX (2.5%) with other excipients such as leucine, MgSt and lactose (Inhalac 120) were manufactured by a validated hand mixing method (Islam et al., 2004b). The formulation ingredients and their ratios in mixtures are presented in Table 1. The micronized drug and ingredients were mixed vigorously for 15 min using glass beads, ensuring breaking of agglomerates during mixing, which produced a ball-milling effect. The capsules (size 3) were filled manually with the weight of 35 ± 2 mg each. The homogeneity was determined for mean drug content and variation within mixtures. 20 mg of each powder mixture was dissolved in 100 mL of solvent and 20 samples were analyzed using a validated HPLC method. The powder mixtures were considered as homogeneous when an average drug content within 100 ± 5 % (mean ± standard deviation) of the theoretical value and a coefficient of variation of less than 5% was obtained (Crooks and Ho, 1976).

2.4. The solubility studies of the drug in PBS

The solubilization of the EDX was carried out by dissolving excess amount of drug (5 mg in 3 mL of water) in the phosphate buffered saline

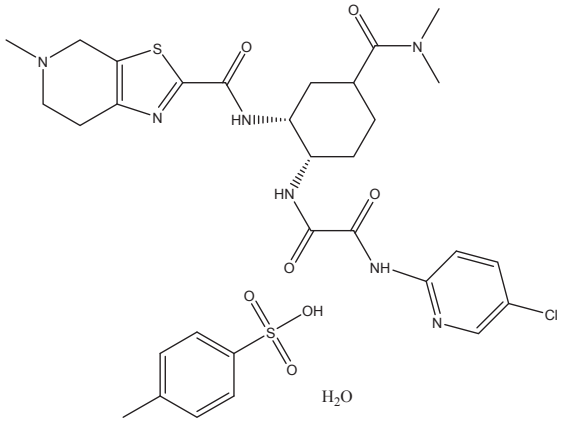

Fig. 1. Chemical structure of Edoxaban tosylate monohydrate.

Table 1
Composition and in-vitro aerosol deposition behaviour of EDX from different formulation mixtures (n = 3).

Formulation blends	RD (%)	ED (%)	FPF (%)	FPD (μg)
EDX only	96.7 ± 1.9	46.8 ± 1.8	11.0 ± 0.7	41.3 ± 1.6
EDX (2.5%) + lactose (F1)	97.6 ± 3.5	78.8 ± 0.8	33.7 ± 0.4	208.0 ± 0.4
EDX (2.5%) + 5% leucine + lactose (F2)	95.7 ± 0.2	81.6 ± 0.6	49.6 ± 0.5	308.7 ± 0.3
EDX (2.5%) + 5% MgSt + lactose (F3)	98.0 ± 1.1	80.4 ± 1.1	45.5 ± 2.1	285.3 ± 0.8
EDX (2.5%) + 2.5 % leucine + 2.5 % MgSt + lactose (F4)	99.0 ± 2.0	82.6 ± 0.2	44.7 ± 0.2	287.7 ± 0.4

(PBS pH 7.3 ± 0.2) and sonicated up to 12 h because of the poor solubility of the drug in PBS. The solution was centrifuged at 16000 rpm for 5 min, supernatant was separated, and the drug was determined using a modified UV- spectrophotometric method (Ravisankar et al., 2018). Briefly, a standard stock solution of EDX was prepared by dissolving 5 mg drug into 50 mL PBS following the ultrasonication for 2 h to confirm the complete dissolution. Using the PBS, the prepared solution was diluted to 30 μg/mL, 20 μg/mL, 10 μg/mL and 4 μg/mL and a calibration plot was obtained. Using this calibration plot, the solubility of the drug in PBS at 6 h and 12 h were determined.

2.5. Plasma clot and turbidity assay

The drug was dissolved in DMSO to prepare a stock solution of 10 μg/mL. Using PBS (pH 7.3 ± 0.2), the stock solution was diluted to obtain 0.25 μg/mL, 0.5 μg/mL, 1.5 μg/mL and 3 μg/mL final concentrations of the drug. The ratio of the DMSO and PBS was 1:99. This solvent mixture (DMSO and PBS) without drug was used as a control. Plasma was extracted from citrated human whole blood taken from the Australian Red Cross Centre (Human ethics approval number 1500000918) by centrifugation at 100 × g for 20 min. 1.0 mL plasma was combined with 30 μL $CaCl_2$ (0.2 M) and 20 μL thrombin (0.5 U/mL). 150 μL of the mix was poured into each sample (96 well-plate) for the turbidity assay. These samples were incubated at 37 °C for 60 min to form clots and read with Clariostar plate reader at 405 nm (Mendhi et al., 2021; Wang et al., 2018; Wolberg et al., 2002). The same experiment was also carried out for the developed EDX DPI formulation. The best two formulations (F3 and F4) were selected to generate robust data on the coagulation activity. 10 mg of powder mixture (formulations) was dissolved in 40 mL of PBS. The solution was centrifuged at 5000 rpm for 20 min. 50 μL of this solution was added to 150 μL plasma for the turbidity assay. The turbidity was measured using a Clariostar plate reader at 405 nm for 60 min and V(max) and maximum turbidity values were determined.

2.6. Scanning electron microscopy (SEM)

The surface morphology of the EDX and its formulations were analysed using SEM (SEM; Tescan Mira3). The samples of drug and its formulations were individually mounted on the metal stubs with the adhesive carbon tape on it. The samples were sprayed with nitrogen using nitrogen gun to clean and prevent contamination. The sample was coated with a conducted 10 nm thick gold layer (Leica, argon gas; pressure 0.5 bar, current 30 mA, coating time 75 s) to avoid surface charge and decrease thermal destruction. It was pulled below high vacuum by identifying secondary electron imaging having an accelerating voltage of 10 kV and a working distance of 8 mm.

2.7. X-ray powder diffraction (XRPD)

The X-ray powder diffraction patterns of above drug formulations and the API phase EDX were collected in Debye-Scherrer geometry (capillary transmission mode) using Rigaku® SmartLab equipped with CuKα (λ = 1.5418 Å) sealed X-ray tube operated at 40 kV and 40 mA. The powder samples were packed into φ 1 mm borosilicate capillaries, which were spun at 15 rpm during data collection. An elliptical primary mirror in CBO-E module was used to focus the X-ray beam to the Hypix3000 detector, which collected diffraction signal over 3.82 °2θ simultaneously, at the same time suppresses CuKβ photons and white radiation background. Both primary and secondary goniometer radii are 300 mm. A 2.5° Soller slit was used on both primary and secondary arms to reduce axial aberration. A 1 mm incident slit was used to just illuminate the capillary. A 15 mm height limiting mask was used resulting in same length of the capillaries measured in goniometer axial direction. On the secondary side, a 6.6 mm anti-scattering slit was placed 50 mm from the capillaries and a 12 mm RS1 slit was placed 185 mm away from the capillary to reduce air scattering background. The X-ray diffraction patterns were collected from 3 to 120 °2θ with step size 0.02 °2θ at a scan speed of 2.0°/min. The deviation of capillary positions from the goniometer centre and instrumental broadening were calibrated using a NIST SRM640 silicon standard.

2.8. DSC/TGA

The thermal properties and decomposition of EDX (original and micronized), and the formulations (F1-F4) were analysed by Differential Scanning Calorimetry (DSC) and Thermo gravimetric analysis (TGA) using concurrent DSC/TGA thermal analyser (NETZSCH STA 449F3). It measures heat flow variation using DSC and mass loss using TGA. 10 mg of sample was placed in a hermetically sealed aluminium pan and all the formulations were scanned from 25 °C to 350 °C at the heating rate of 10 °C/ min. The stability of EDX in the mixtures was confirmed by the characteristic DSC peak, which corresponds to the melting point of EDX.

2.9. ATR-FTIR

The ATR-FTIR spectra of EDX drug and its mixtures were analysed by Alpha-P FTIR with attenuated total reflectance (ATR accessory) (Arthur, 1953014032) (Bruker, Massachusetts, United States) with an angle of incidence of 40 °C and a deuterated triglycine sulphate (DTGS) detector. A small amount of sample was placed on the top of diamond glass and secured using high-pressure clamp. The spectra were collected at a resolution of 8 cm^{-1} and 64 scans were performed in the range of 4000 cm^{-1} to 400 cm^{-1}. It was then analysed by means of the analytical software, OPUS (Bruker, Massachusetts, United States).

2.10. Determination of EDX by HPLC

Using a modified HPLC method (Ravisankar et al., 2021), the drug was analysed in all formulations. The separation was carried out using Agilent HPLC Series 1100 with Column heater and Fluorescence Detector (Heracles) Hewlett-Packard (Waldbronn, Germany). Agilent column (4 μm Poroshell 120, EC-C18, 4.6 × 250 mm) and a guard column (4 μm, California, United States). The mobile phase composition was 0.1 % formic acid water and acetonitrile (*v/v* 80:20), and flow rate was 1.00 mL/min at a total run time of 10 min. The autosampler was used for 20 μL injection for each sample. A calibration curve was plotted at concentrations ranging from 0.25 μg/mL to 100 μg/mL and the limit of quantification (LOQ) was 0.25 μg/ml. All the samples were prepared and filtered before use. The HPLC was operated using Value Solution ChemStation software.

2.11. In-vitro aerosolization of powder blends

The characterization of EDX DPI formulation blends was done by in-vitro aerosolization by using a twin stage impinger (TSI). The capsules (size 3) were filled manually with the powder formulation weighing 30–32 mg each. For drug only formulation, approximately 800 μg of the

micronized EDX (equivalent to the amount of EDX in 30 to 32 mg of the 2.5% mixture) was poured into each capsule. The commercially available inhalation device, Breezhaler® (Novartis Pharmaceuticals Pvt Ltd, NSW, Australia) was used to aerosolize powder from the formulations. The stage 1 (S1) and stage 2 (S2) of TSI contained 7 mL and 30 mL of solvent (0.1 % formic acid water and acetonitrile, *v/v* 80:20), respectively. The airflow was drawn at the flow rate of 60 ± 5 L /min at the mouthpiece before each measurement through TSI using the vacuum pump. The cut-off diameter of S2 was 6.4 μm. After each run, all the sections i.e., the device (Breezhaler®) S1 and S2 were washed with the solvent. The deposition of the drug particles at various stages of TSI was determined using a validated HPLC method. The drug deposition of EDX was determined using the following parameters: the recovered dose (RD), the emitted dose (ED) and the fine particle fraction (FPF) (Steckel and Müller, 1997). RD is the total amount of drug collected from the Breezhaler®, S1 and S2 of TSI. ED is the amount of drug exiting the device, deposited into S1 and S2, and presented as a percentage of RD. The FPF is the amount of drug deposited in the lower stage (S2) of TSI and presented as the percentage of ED. FPD is the mass of the drug particles deposited in the stage 2 of the TSI.

2.12. Statistical analysis

The statistical analysis was completed by applying one-way analysis of variance (ANOVA). P values of $p < 0.05$ were considered as significant difference. All measurements were taken in triplicate and expressed as mean values and standard deviations.

3. Results and discussion

3.1. Formulation mixtures and homogeneity test

The DPI formulations of EDX were prepared with large lactose, leucine and magnesium stearate at different concentrations (Table 1). These mixtures showed excellent homogeneity as the mean EDX contents were within 100 ± 4% and the coefficient of variation < 2%. This results are supported by other studies carried out in our laboratory using different drugs (Rashid et al., 2019).

3.2. Particle size by laser diffraction

The micronized particle was reduced to the required particle size of < 5 μm, which was confirmed by laser diffraction technique using a Master sizer. The size and size distributions of micronized EDX represented by Fig. 2, showed that the mean particle size was 3.1 ± 1 μm (n = 3) which demonstrated that the micronized EDX particles were inhalable size. Therefore, the prepared EDX particles were used in making the DPI formulations for other experiments in this study.

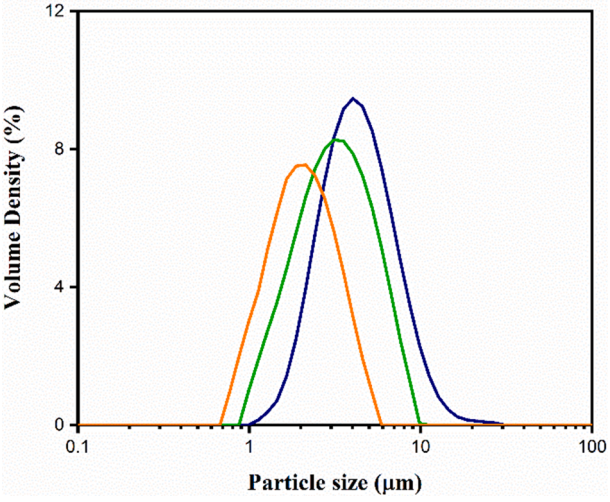

Fig. 2. Average particle size measurement of EDX using Master sizer 3000 (n = 3).

3.3. SEM

The SEM images in Fig. 3 show the morphology of original drug and the formulations. The images of the original EDX (Fig. 3A) and the micronized particles (Fig. 3 B) clearly showed that the micronized particles are small (<5μm) and remained as agglomerated form. The SEM images of formulations F1 to F4 (Fig. 3 C-F) showed that the small drug particles are adhered on the surface of lactose particles (inset Fig. 3F4) along with the excipients such as MgSt and Leucine which were used as ternary agents to enhance the dispersibility.

3.4. XRPD –Identification of EDX crystallinity

The X-ray Powder Diffraction pattern of the EDX used in this study is shown in Fig. 4. The intensity axes of all the XRPD patterns are displayed to highlight the small peaks. This relative new drug phase was not included in either ICDD PDF-4 Organic 2020, CCDC database, or COD database. To date, no crystal structure of EDX was published elsewhere. Phase confirmation was done by matching the measured XRPD pattern with a XRPD pattern reported in an European patent EP3318568A1 (Berenguer Maimó et al., 2016) of EDX as shown in Fig. S1. It is, therefore, suggested that the EDX used in this study is in the form of tosylate monohydrate.

The XRPD patterns of the EDX before and after micronizing are compared in Fig. 4 and it is clear that the crystallite size of EDX was reduced by grinding, due to the obvious broadening of all the diffraction peaks. The crystallite sizes of EDX crystals before and after micronizing was quantified using Pawley refinement of the above indexed unit cell. The refined crystallite size reduced from 145(2) nm to 59.9(4) nm. The small crystal size of API could expedite the drug dissolution from the formulation

3.5. XRPD – Quantitative phase analysis using PONKCS method

Using Partially Or No Known Crystal Structure (PONKCS method), the amount of EDX was quantified in the formulation (F1-F4). Initially, the product of unit cell mass and unit cell volume can be experimentally calibrated according to a standard mixture with known weight percent of internal standard (Scarlett and Madsen, 2006). The intensity of each *hkl* reflections from Pawley fittings of the original EDX was fixed in order to calibrate the unit cell mass "ZM factor" of this PONKCS model according to the 1:1 wt% mixture of the edoxaban tosylate monohydrate and α-lactose monohydrate. Unit cell volume was calculated from the refined lattice parameters. The calibrated PONKCS model was then used to quantify the EDX content in the formulations. Fig. 5 represents the Rietveld quantification of the formulation F3 and Fig. S3 contains the QPA of Formulation F1, F2 and F4 and Table S1. Using the PONKCS model, the quantification of crystal structures of α-lactose monohydrate, L-Leucine, and magnesium stearate in the mixture of meropenem was previously reported (Muneer et al., 2020) and very similar data are obtained in the formulations containing EDX.

3.6. DSC-TGA

Fig. 6 contains the thermograms of DSC and TGA of EDX API, micronized EDX, lactose monohydrate and all formulations F1 to F4. The DSC thermograms of both original and micronized EDX show two peaks at 252 °C and 270 °C which refer to the melting points of the salt form of EDX (Fig. 6 A and B). This outcome revealed that the micronization process did not affect the crystallinity of the drug as there are no weight loss by TGA (%) at the same temperature. The mixtures of drug with the

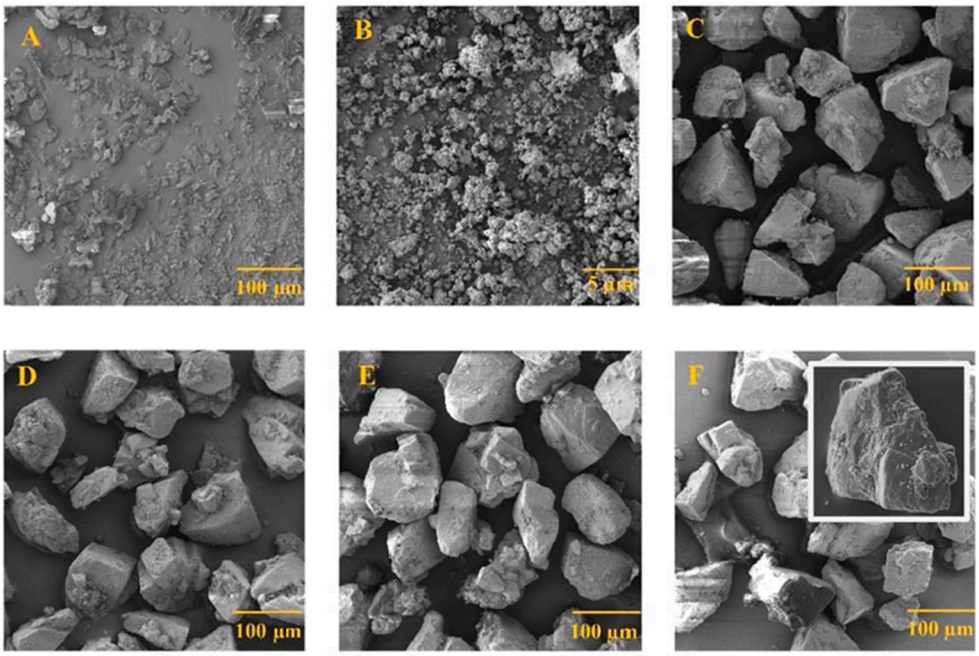

Fig. 3. SEM images of the (A) EDX, (B) micronized EDX, (C) F1: EDX + Lac, (D) F2: EDX + Leu + Lac, (E) F3: EDX + MgSt + Lac, and (F) F4: EDX + MgSt + Leu + Lac (inset photo represents drug/excipients are adhered on the surface of large lactose carrier).

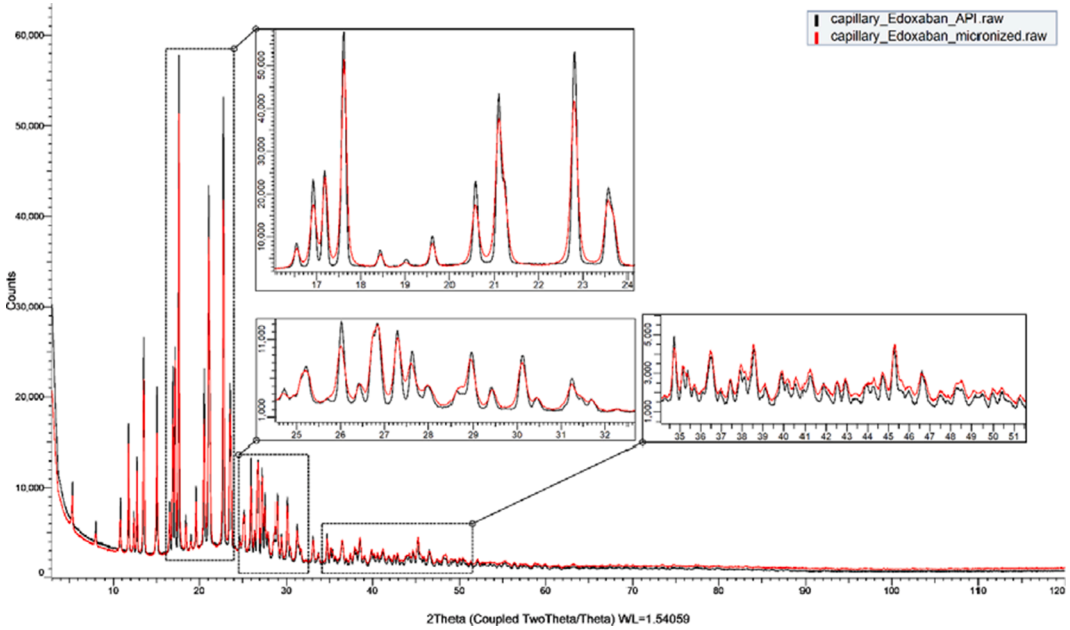

Fig. 4. Evaluation of XRPD patterns of EDX before and after micronizing.

excipients show the characteristic peaks at 150 °C and 217 °C for lactose monohydrate (Fig. 6 C), which is supported by others (Rashid et al., 2019). The amount of drug in the formulation was very low (2.5%) and that's why the characteristic peaks for drug in the formulations are not visible.

3.7. ATR-FTIR

The FTIR showed distinct peaks of EDX at 1618 cm^{-1} and 1500 cm^{-1}, which corresponds to the band stretching of C═O of the amide group and the C═C, respectively (Wang et al., 2017). The peaks at 1375 cm^{-1}, 1217 cm^{-1}, 1158 cm^{-1}, 1010 cm^{-1} are attributed to —CH_3 symmetrical deformation. The peak at 684 cm^{-1} is due to CH out of plane aromatic band. There is no shift or change in characteristic peaks of EDX before and after micronization as seen in Fig. 7 (A). After formulation development with excipients, the characteristic peaks at 1618 cm^{-1} (C═O), 1500 cm^{-1} (C═C did not change which refers to the stability of the drug EDX in the powder mixtures and no evidence of drug-excipient interaction Fig. 7 (B) (Debnath et al., 2017).

3.8. In-vitro aerosolization performance

The RD, ED, FPF and FPD are presented the Table 1. The RDs for all formulations are between 95 and 99%; however, the EDs were between

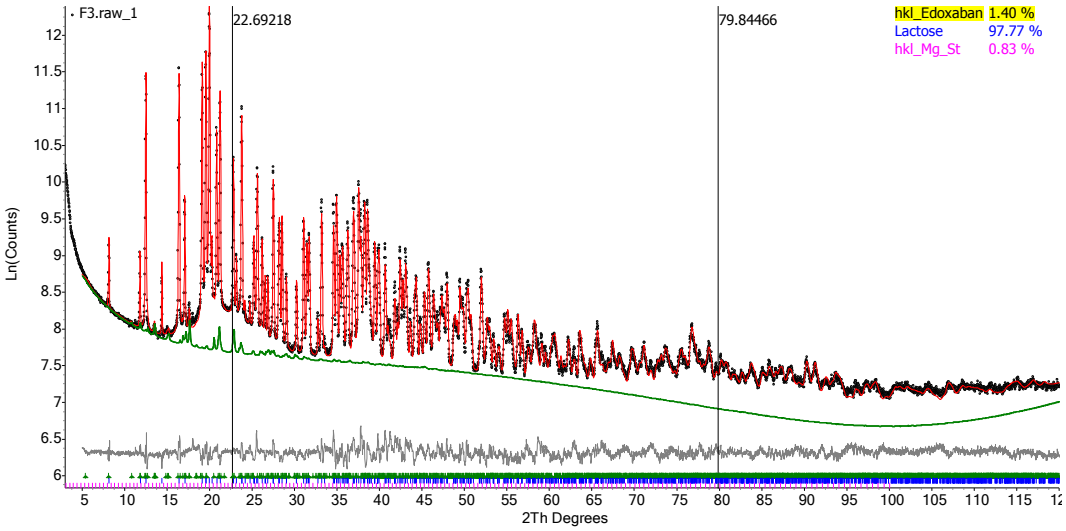

Fig. 5. Rietveld Quantification of the formulation F3 with the contribution of API phase highlighted.

78 and 83%. Although the EDs of the prepared formulations are low, similar outcomes are demonstrated by others (Larhrib et al., 2003). It is unclear about the reason behind the lack of increase in the EDs after mixing with the flow promoters like leucine and MgSt in the formulations. The FPF of the EDX API only was 4.9 % and indicative of very poor performance. The addition of lactose in F1 increased the FPF to 33.7% which is significantly high ($p < 0.05$). The increase in the FPF after mixing the drug with the excipients (F1 to F4) is due to the improved drug flow caused by the reduced cohesion of drug particles in presence of large carrier lactose particles. Adding the leucine and MgSt as ternary agents in the formulations may reduce drug carrier adhesion by the fine leucine and MgSt particles occupying the binding sites at the lactose carrier particles thereby making easy detachment of drug particles during aerosolization (Jones et al., 2008). These excipients also act as the flow promoter of the micronized EDX particles. As a result, the FPF, RD and ED increased for the formulation F2, F3 and F4 due to this property of the fine ternary particles. The FPF for F2, F3 and F4 are 49.6%, 45.5%, and 44.7% respectively. This shows that all the excipients used in the formulations either alone or in combination produced improved FPD in all the developed formulations and significantly higher ($p < 0.05$) than the API of EDX alone. Therefore, these excipients are compatible with the drug EDX and can be utilized to develop stable DPI formulations.

3.9. Solubility studies of EDX in PBS

Using a UV-spectrophotometric method, the solubility of the active drug in PBS (pH 7.3 ± 0.2) was determined as 63 μg/mL and 98.8 μg/mL in 6 and 12 h, respectively. This reveals that the drug is poorly soluble in PBS. As the PBS was used as the main solvent for coagulation study, the outcomes of the solubility of EDX in PBS directed us to use DMSO (PBS: DMSO was 99:1) for complete dissolution of the drug from the formulation in short period time. This solution was diluted and completed the turbidity experiments as demonstrated below (Section 3.9).

3.10. Effect of EDX DPI formulation on coagulation

Turbidity assays were performed to evaluate the clotting process. It was noted that the clot turbidity steadily increased in all samples, with the highest values attained in the control samples; however, there was a substantial decline in the maximum turbidity as the concentration of the drug was increased compared to the control sample (Fig. 8 A). There was a considerable increase in the V(max) values, as V(max) is inversely proportional to the slope values (Fig. 8 B and C), of the results indicate reduced clotting rates with increasing drug concentration. The highest maximum turbidity was obtained with the control samples and decreased with increasing drug concentrations indicating the change in clot structure due to the impact of the drug.

In general, clot turbidity measurements can offer evidence about clot formation and structure (Gidley et al., 2018; Gould et al., 2015; Litvinov et al., 2019; Pieters et al., 2018; Posch et al., 2020; Zucker et al., 2014). Previous studies that co-link Thromboelastography (TEG) analysis with turbidity measurements have shown that clot strength and turbidity are inversely proportional (Zeng et al., 2020). It is also evident that the clots with higher turbidity values indicate thinner fibre diameter with tighter clot structures (Chan et al., 2015; Mendhi et al., 2021). Therefore, based on this evidence, it can be inferred that the drug displayed properties to reduce coagulation rates and alter the clot structure at a very low dose.

The DPI formulations of EDX showed a significant anticoagulation effect (Fig. 9 A). As demonstrated, pulmonary coagulopathy, as well as cerebral thromboembolism, are common problems associated with COVID-19 infection, which are currently treated by oral or parenteral anticoagulants. Direct anticoagulants delivery was suggested as a safe and effective treatment option in selected COVID-19 patients who have suffered from venous thromboembolism (Kartsios et al., 2021). The bioavailability of EDX from the currently available oral dose (60 mg/daily) is 256 ± 88 ng/mL obtained in 1–3 h after administration (Parasrampuria and Truitt, 2016). Sugiyama et al. (Sugiyama et al., 2020) found reduced thrombosis with patients suffering from COVID-19 infections developed cerebral venous thrombosis along with pulmonary thromboembolism after oral administration of EDX at a dose of 60 mg/day, which is a very high dose and associated with bleeding. Our developed EDX DPI formulations produced FPD between 208 and 309 μg (Table 1). In our in-vitro study, the predicted C_{max} values are calculated based on the fine particle dose (FPD, Table 1) of the aerosolized EDX from the DPI formulations. It is assumed that all drug particles deposited into deep lungs will be absorbed and therefore, the desired therapeutic concentration of 256 ng/mL (0.26 μg/mL) obtained from 60 mg of orally administered EDX could be achieved by inhaling the developed EDX DPI formulation from where 208–309 μg (Table 1, FPD) of EDX would be expected to be deposited into deep lungs for absorption. The coagulation data shows that the calculated plasma concentration of the drug from DPI formulations will produce significant anticoagulation in 10–20 min (Fig. 9A) at a very low concentration. Therefore, it is suggested that the developed EDX DPI formulation will produce the desired plasma drug concentration at a very low dose. It can be concluded that the inhaled EDX formulation can be used for the efficient treatment of pulmonary or cerebral coagulopathy associated with COVID 19 infection at a very low

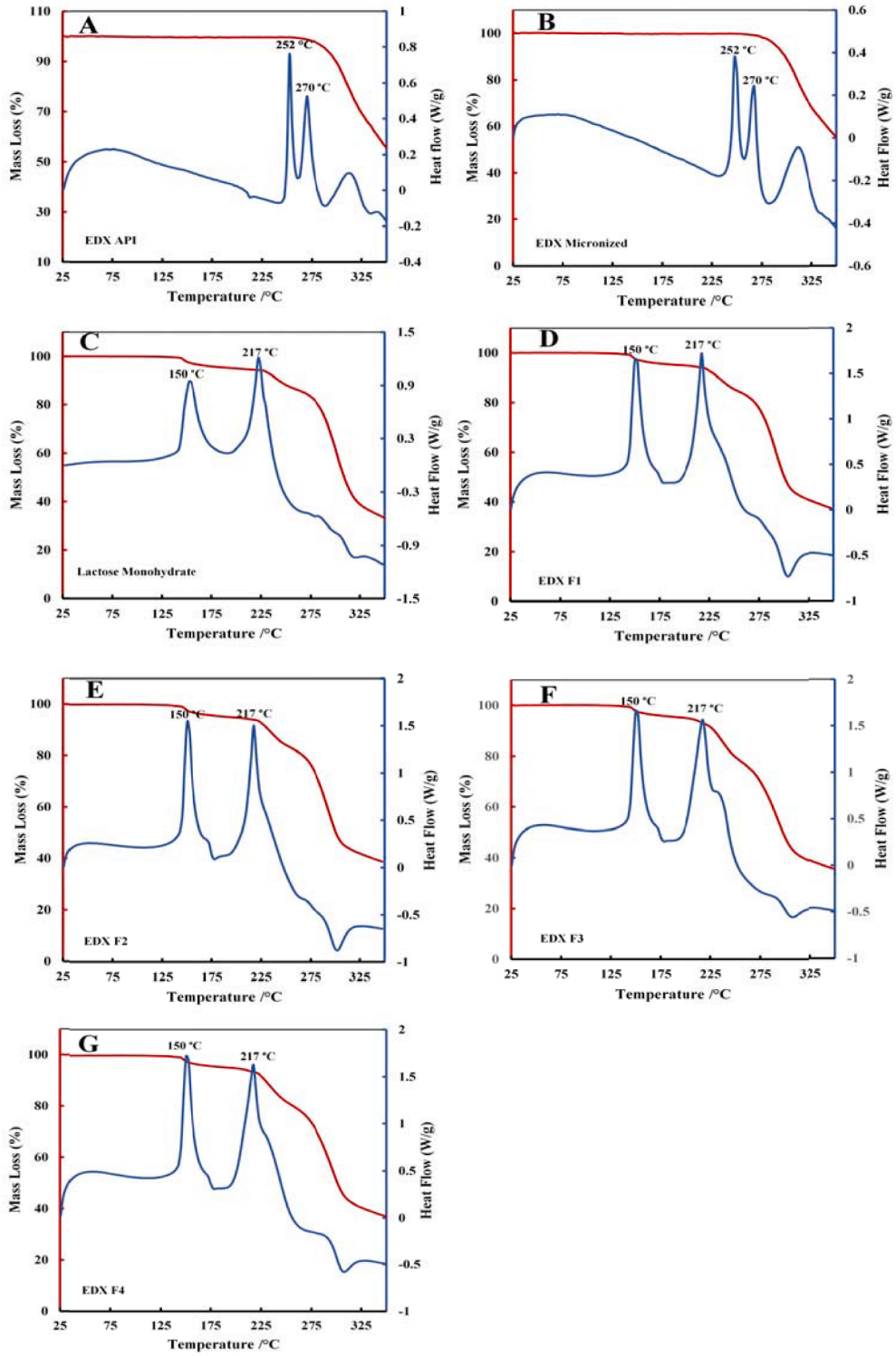

Fig. 6. DSC/ TGA thermograms of EDX and its formulation mixtures (A) original EDX, (B) micronized EDX (C) Lactose monohydrate, (D) F1, (E) F2, (F) F3, (G) F4.

dose. Although the developed EDX is a DPI formulation, it can be formulated as a metered-dose inhaler (MDI) and solutions for nebulization. The DPI and MDIs can be useful for the patients who are under quarantine at home/ hotel or hospital; however, the nebulised solution can be used for the aged patients who are terminally ill or under ventilation.

Vaccination against COVID 19 infection is progressing around the world; however, the vaccine manufactured by Astra Zeneca showed blood clot (thrombocytopenia) and leading to the death of some patients. Therefore, some countries have banned the use of Astra Zeneca vaccine. As our developed EDX formulation showed a promising in-vitro anticoagulation effect, we suggest this formulation may be of benefit to the patients who are suffering from pulmonary or cerebral coagulopathy; however, further studies are warranted to get a better understanding on the clinical application of the inhaled EDX formulation. Overall, this is the first-time investigation on the in-vitro anticoagulation of the inhaled EDX formulation with a promising outcome. We believe this study has opened a new window for the management of

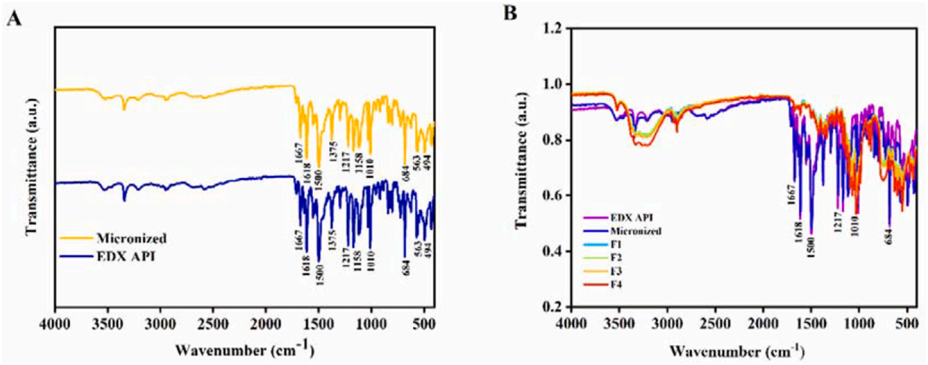

Fig. 7. FTIR of EDX (A) EDX API and micronized, (B) formulation mixtures (F1-F4).

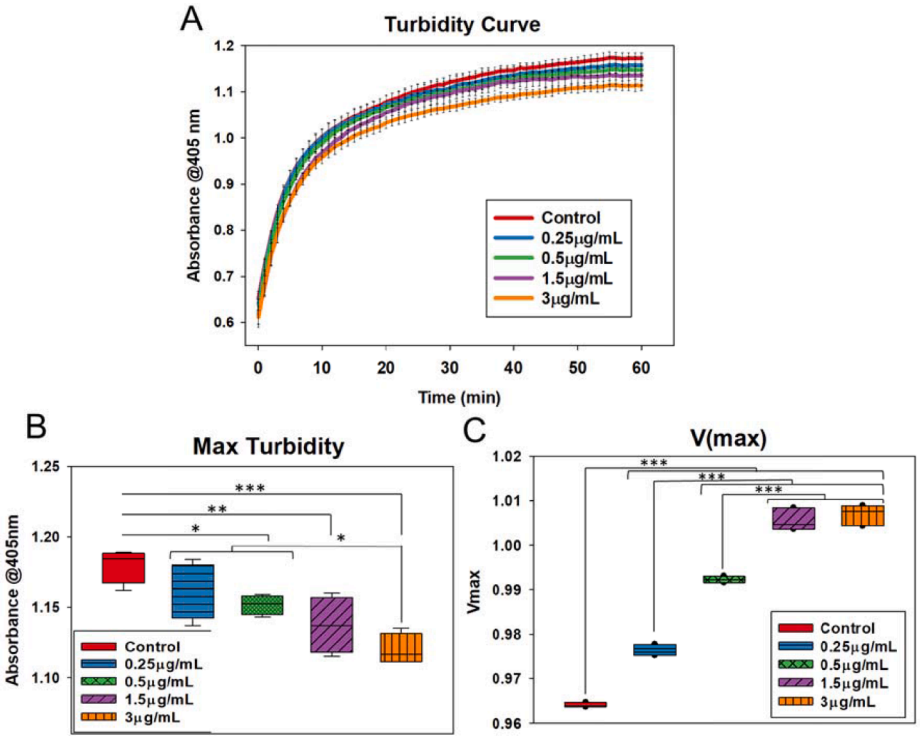

Fig. 8. (A) OD values indicating steady increase in turbidity values over a period of 60 min. The control samples displayed the highest level of turbidity. (B) V(max) values were calculated to find the clotting rates. Control samples showed the lowest V(max) values, and values increased with increasing drug concentration, indicating slowing down of clotting with increasing drug concentration. (C) Maximum turbidity values were plotted. Control samples showed the highest maximum turbidity with decreasing turbidity with an increase in drug concentration, indicating reduced clotting with the addition of drug. Error bars show the standard deviation of three different samples. Blackline represents mean, and whiskers imply standard deviation in all box plots.

pulmonary or cerebral coagulopathy associated with COVID 19 infection. We suggest that the inhaled EDX would produce better therapeutic activity for the management of coagulopathy at a very low dose.

4. Conclusion

This study demonstrates a novel inhaled DPI formulation of EDX for the management of coagulopathy associated with COVID-19 infection. Various excipients were used in developing the DPI formulation and no drug-excipient interactions were observed. This confirmed the compatibility of these excipients used in the preparation of various formulations with the drug. The FTIR and Raman are useful techniques for characterizing the drug excipients interactions and the structural integrity of the drug in the formulations. The in-vitro aerosolization of the drug characterised as the FPF of the formulations were promising. The observed FPF of EDX in the developed DPI formulations are comparable to some commercial DPI products of other drugs. The developed formulations showed a very promising in-vitro anticoagulation effect at a concentration of 3 µg/mL within 10–20 min. To date, this is the first study to investigate the inhaled EDX DPI formulation for anticoagulation effect. This innovative study demonstrated a promising strategy to resolve an emerging health problem and have a major impact on health research. The mortality rate due to fatal COVID-19 disease, which destroys lung function, has increased and currently, no inhaled formulations are available. Therefore, the outcome of this study might be useful in addition to other drugs for the treatment of coagulopathy associated with COVID-19 infection. Further studies are warranted to investigate the toxicity and clinical application of the inhaled EDX formulations.

CRediT authorship contribution statement

Md. Abdur Rashid: Data curation, Formal analysis, Funding acquisition, Investigation, Methodology, Project administration, Resources, Writing – original draft. **Saiqa Muneer:** Data curation, Formal analysis, Investigation, Methodology, Writing – original draft. **Jayanti Mendhi:** Data curation, Formal analysis, Investigation, Methodology, Writing – original draft. **Mohammad Zaidur Rahman Sabuj:** Data curation, Investigation, Methodology, Writing – original draft. **Yahya Alhamhoom:** Funding acquisition, Project administration, Resources, Writing – review & editing. **Yin Xiao:** Conceptualization, Resources,

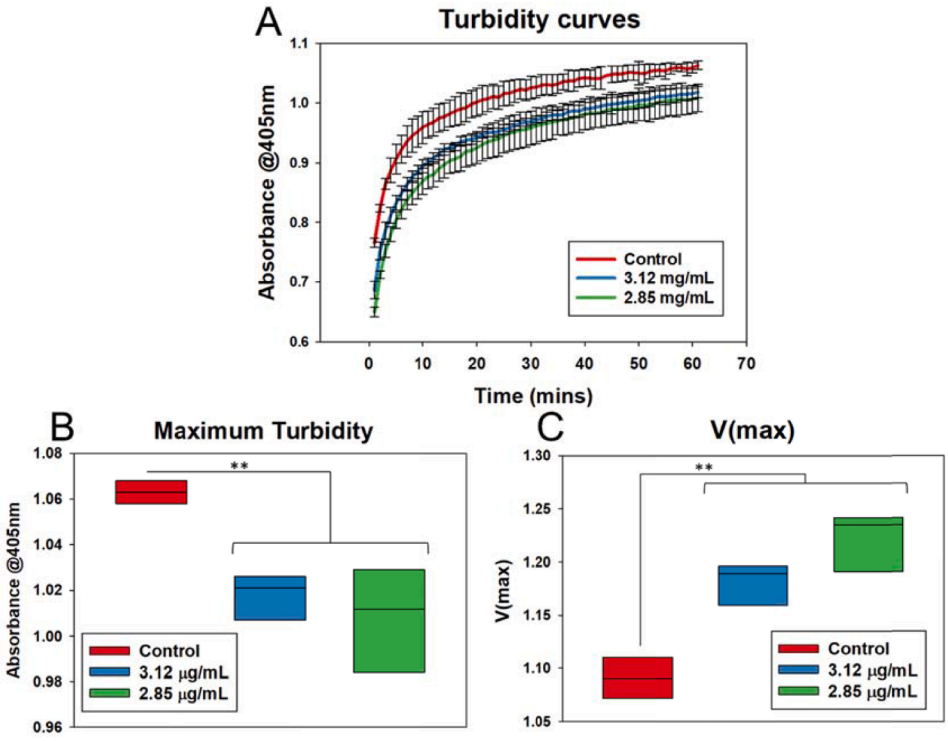

Fig. 9. (A) OD values indicating steady increase in turbidity values over a period of 60 min for the formulations. The control samples displayed the highest level of turbidity. (B) Maximum turbidity values were plotted. Control samples showed increased maximum turbidity compared to the formulations and no significant difference between the formulations indicating reduced clotting with the formulations. (C) V(max) values were calculated to find clotting rates. Control samples showed lowest V(max) values and there was no significant difference in the V(max) values of the formulations. Black line represents mean in all box plots. P values: *p < 0.05, **p < 0.01, ***p < 0.001.

Supervision, Validation, Writing – review & editing. **Tony Wang:** Data curation, Formal analysis, Methodology, Writing – original draft. **Emad L. Izake:** Conceptualization, Resources, Supervision, Validation, Writing – review & editing. **Nazrul Islam:** Conceptualization, Formal analysis, Project administration, Resources, Supervision, Validation, Writing – review & editing.

Declaration of Competing Interest

The authors declare that they have no known competing financial interests or personal relationships that could have appeared to influence the work reported in this paper.

Acknowledgement

The authors thank the Deanship of Scientific Research at King Khalid University (Abha, Saudi Arabia) for funding this work through General Research Project under grant number (G.R.P. 138). The authors extend their thanks to Queensland University of Technology (Brisbane, Australia) for granting access to the Central Analytical Research Facility (CARF).

List of chemicals studied in this article

Edoxaban, PBS, lactose, leucine, magnesium stearate, plasma, thrombin, formic acid and acetonitrile.

Appendix A. Supplementary material

Supplementary data to this article can be found online at https://doi.org/10.1016/j.ijpharm.2021.121122.

References

Berenguer Maimó, R., Racamonde Villanueva, M., Winter, S.B.D., 2016. In: Preparation process of edoxaban tosylate monohydrate. European Patent Office, Spain, p. 18.

Chan, H.-K., Clark, A., Gonda, I., Mumenthaler, M., Hsu, C., 1997. Spray dried powders and powder blends of recombinant human deoxyribonuclease (rhDNase) for aerosol delivery. Pharm. Res. 14, 431–437.

Chan, L.W., Wang, X., Wei, H., Pozzo, L.D., White, N.J., Pun, S.H., 2015. A synthetic fibrin cross-linking polymer for modulating clot properties and inducing hemostasis. Sci. Transl. Med. 7, 277ra29.

Costanzo, L., Palumbo, F.P., Ardita, G., Antignani, P.L., Arosio, E., Failla, G., Disorders, L., 2020. Coagulopathy, thromboembolic complications, and the use of heparin in COVID-19 pneumonia. 8, 711–716.

Crooks, M.J., Ho, R., 1976. Ordered mixing in direct compression of tablets. Powder Technol. 14 (1), 161–167.

Debnath, S.K., Saisivam, S., Omri, A., 2017. PLGA Ethionamide nanoparticles for pulmonary delivery: Development and in vivo evaluation of dry powder inhaler. J. Pharm. Biomed. Anal. 145, 854–859.

Ferreira, J., Mirco, A.J., 2015. Systematic review of cost-effectiveness analyses of novel oral anticoagulants for stroke prevention in atrial fibrillation. 34, 179–191.

Flam, B., Wintzell, V., Ludvigsson, J.F., Mårtensson, J., Pasternak, B.J., 2021. Direct oral anticoagulant use and risk of severe COVID-19. 289, 411-419.

Fogarty, H., Townsend, L., Ni Cheallaigh, C., Bergin, C., Martin-Loeches, I., Browne, P., Bacon, C.L., Gaule, R., Gillett, A., Byrne, M., 2020. COVID19 coagulopathy in Caucasian patients. Br. J. Haematol. 189 (6), 1044–1049.

Gidley, G.N., Holle, L.A., Burthem, J., Bolton-Maggs, P., Lin, F.-C., Wolberg, A.S., 2018. Abnormal plasma clot formation and fibrinolysis reveal bleeding tendency in patients with partial factor XI deficiency. Blood Adv. 2, 1076–1088.

Gould, T.J., Vu, T.T., Stafford, A.R., Dwivedi, D.J., Kim, P.Y., Fox-Robichaud, A.E., Weitz, J.I., Liaw, P.C., 2015. Cell-free DNA modulates clot structure and impairs fibrinolysis in sepsis. Arterioscler. Thromb. Vasc. Biol. 35, 2544–2553.

Hippensteel Joseph, A., LaRiviere Wells, B., Langouet-Astrie Christophe, J., Schmidt Eric, P., LaRiviere Wells, B., Colbert James, F., Schmidt Eric, P., 2020. Heparin as a therapy for COVID-19: current evidence and future possibilities. Am. J. Physiol. Lung Cell Mol. Physiol. 319, L211–L217.

Islam, N., Rahman, S., 2021. Novel Pulmonary Delivery of Antiviral Drugs for Treating COVID-19 in Patients with Parkinson's Disease. Current Drug Delivery.

Islam, N., Stewart, P., Larson, I., Hartley, P., 2004a. Effect of carrier size on the dispersion of salmeterol xinafoate from interactive mixtures. 93, 1030–1038.

Islam, N., Stewart, P., Larson, I., Hartley, P. 2004b. Lactose surface modification by decantation: are drug-fine lactose ratios the key to better dispersion of salmeterol xinafoate from lactose-interactive mixtures? 21, 492–499.

Jones, M.D., Hooton, J.C., Dawson, M.L., Ferrie, A.R., Price, R., 2008. An investigation into the dispersion mechanisms of ternary dry powder inhaler formulations by the quantification of interparticulate forces. Pharm. Res. 25, 337–348.

Kartsios, C., Lokare, A., Osman, H., Perrin, D., Razaq, S., Ayub, N., Daddar, B., Fair, S., Thrombolysis, 2021. Diagnosis, management, and outcomes of venous thromboembolism in COVID-19 positive patients: a role for direct anticoagulants? 51, 947–952.

Kearon, C., Akl, E.A., Comerota, A.J., Prandoni, P., Bounameaux, H., Goldhaber, S.Z., Nelson, M.E., Wells, P.S., Gould, M.K., Dentali, F.J.C., 2012. Antithrombotic therapy for VTE disease: antithrombotic therapy and prevention of thrombosis: American

College of Chest Physicians evidence-based clinical practice guidelines. 141, e419S-e496S.
Larhrib, H., Martin, G.P., Marriott, C., Prime, D., 2003. The influence of carrier and drug morphology on drug delivery from dry powder formulations. Int. J. Pharm. 257, 283–296.
Litvinov, R.I., Nabiullina, R.M., Zubairova, L.D., Shakurova, M.A., Andrianova, I.A., Weisel, J.W., 2019. Lytic Susceptibility, Structure, and Mechanical Properties of Fibrin in Systemic Lupus Erythematosus. Front. Immunol. 10.
Matsushima, N., Lee, F., Sato, T., Weiss, D., Mendell, J., 2013. Bioavailability and safety of the factor Xa inhibitor edoxaban and the effects of quinidine in healthy subjects. 2, 358–366.
Mendhi, J., Prasadam, I., Subramaniam, S., Bai, L., Gao, W., Batra, J., Crawford, R., Yang, Y., Xiao, Y., 2021. Nitric Oxide generating coating alters hematoma structure and soft tissue healing. Appl. Mater. Today 22, 100919.
Muneer, S., Wang, T., Rintoul, L., Ayoko, G.A., Islam, N., Izake, E., 2020. Development and characterization of meropenem dry powder inhaler formulation for pulmonary drug delivery. 587, 119684.
Parasrampuria, D.A., Truitt, K., 2016. Pharmacokinetics and pharmacodynamics of edoxaban, a non-vitamin K antagonist oral anticoagulant that inhibits clotting factor Xa. 55, 641–655.
Patel, R., Czuprynska, J., Roberts, L.N., Vadher, B., Rea, C., Patel, R., Gee, E., Saul, G., Coles, E., Brown, A., 2021. Switching warfarin patients to a direct oral anticoagulant during the Coronavirus Disease-19 pandemic. 197, 192–194.
Pieters, M., Philippou, H., Undas, A., de Lange, Z., Rijken, D.C., Mutch, N.J., 2018. An international study on the feasibility of a standardized combined plasma clot turbidity and lysis assay: communication from the SSC of the ISTH. J. Thromb. Haemost. 16, 1007–1012.
Posch, F., Hofer, S., Thaler, J., Hell, L., Königsbrügge, O., Grilz, E., Mauracher, L.-M., Gebhart, J., Marosi, C., Jilma, B., 2020. Ex vivo properties of plasma clot formation and lysis in patients with cancer at risk for venous thromboembolism, arterial thrombosis, and death. Transl. Res. 215, 41–56.
Prime, D., Atkins, P.J., Slater, A., Sumby, B., 1997. Review of dry powder inhalers. Adv. Drug Deliv. Rev. 26, 51–58.
Rashid, M.A., Elgied, A.A., Alhamhoom, Y., Chan, E., Rintoul, L., Allahham, A., Islam, N., 2019. Excipient interactions in glucagon dry powder inhaler formulation for pulmonary delivery. Pharmaceutics 11, 207.
Ravisankar, P., Srikanth, D., Reddy, C.V., Rao, P.R., Babu, P.S., 2018. Development and validation of UV spectrophotometric method for the determination of Edoxaban Tosylate Monohydrate in pharmaceutical dosage form. Indian J. Res. Pharm. Biotechnol. 6 (2), 73–78.
Ravisankar, P., Eswarudu, M.M., Sivakrisnan, P., Srikanth, D., Srinivash Babu, P., Rohit, N., 2021. Novel RP-HPLC method fo determination of Edoxaban tosylate monohydrate in bulk and its pharmaceutical dosage form. J. Pharmaceut. Sci. Res. 13 (5), 232–237.
Rentsch, C.T., Beckman, J.A., Tomlinson, L., Gellad, W.F., Alcorn, C., Kidwai-Khan, F., Skanderson, M., Brittain, E., King, J.T., Ho, Y.-L.J.b., 2021. Early initiation of prophylactic anticoagulation for prevention of coronavirus disease 2019 mortality in patients admitted to hospital in the United States: cohort study. 372.
Scarlett, N.V.Y., Madsen, I.C., 2006. Quantification of phases with partial or no known crystal structures. Powder Diffr. 21, 278–284.
Steckel, H., Müller, B.W., 1997. In vitro evaluation of dry powder inhalers II: influence of carrier particle size and concentration on in vitro deposition. Int. J. Pharm. 154, 31–37.
Sugiyama, Y., Tsuchiya, T., Tanaka, R., Ouchi, A., Motoyama, A., Takamoto, T., Hara, N., Yanagawa, Y., 2020. Cerebral venous thrombosis in COVID-19-associated coagulopathy: A case report. 79, 30–32.
Tang, N., Bai, H., Chen, X., Gong, J., Li, D., Sun, Z., 2020. Anticoagulant treatment is associated with decreased mortality in severe coronavirus disease 2019 patients with coagulopathy. J. Thromb. Haemostasis 18, 1094–1099.
Wang, H., George, G., Bartlett, S., Gao, C., Islam, N., 2017. Nicotine hydrogen tartrate loaded chitosan nanoparticles: Formulation, characterization and in vitro delivery from dry powder inhaler formulation. Eur. J. Pharm. Biopharm. 113, 118–131.
Wang, X., Luo, Y., Yang, Y., Zheng, B., Yan, F., Wei, F., Friis, T.E., Crawford, R.W., Xiao, Y., 2018. Alteration of clot architecture using bone substitute biomaterials (beta-tricalcium phosphate) significantly delays the early bone healing process. J. Mater. Chem. B 6, 8204–8213.
Wells, P.S., Holbrook, A.M., Crowther, N.R., Hirsh, J., 1994. Interactions of warfarin with drugs and food. 121, 676–683.
Wolberg, A., Gabriel, D., Hoffman, M., 2002. Analyzing fibrin clot structure using a microplate reader. Blood Coagulation Fibrinolysis: Int. J. Haemostasis Thrombosis 13, 533–539.
Zeng, Z., Fagnon, M., Chakravarthula, T.N., Alves, N.J., 2020. Fibrin clot formation under diverse clotting conditions: Comparing turbidimetry and thromboelastography. Thromb. Res. 187, 48–55.
Zucker, M., Seligsohn, U., Salomon, O., Wolberg, A.S., 2014. Abnormal plasma clot structure and stability distinguish bleeding risk in patients with severe factor XI deficiency. J. Thromb. Haemost. 12, 1121–1130.